Original Research Article
μ-Synthesis of an under-actuatedbridge crane

ABSTRACT

During crane operation, the distribution of load mass may be nonuniform, which leads to the model uncertainty of the crane.Additionally, external disturbances such as wind and friction can cause oscillation of crane loads. A robust control strategy is proposed for an uncertain bridge crane system to address these issues. This strategy aims to accurately locate, quickly transport, and suppressits swing angle. The bridge crane is firstmodeled as the twodegree-of-freedom system to study the control problem, and the load mass and the track friction coefficients are taken as parameter uncertainties.The appropriate performance weight and input weight functions are then designed for the closed-loop system by a concluded procedure.The relationship between the weight-function parameters and the resulting performance is analyzed. According to these weight functions, a μ-synthesis robust controller is designed using the DK-iteration algorithm. The output disturbance is introduced to analyze the pendulum angle suppression and perturbationrejection abilities of the closed-loop system in a shorterperiod. Finally, the effectiveness of the designed control method is verified by a simulation example.

Keywords: Under-actuated; μ-Synthesis; Bridge crane; Robust control.

1. INTRODUCTION

Overhead cranes are a type of lifting and loading transportation equipment that is capable of moving in three directions. They are commonly used in various settings, such as ports, workshops, and other industrial locations. The horizontal bridge of the crane is supported by two legs, giving it a gantry shape. The lifting trolley runs on the bridge horizontally and uses a steelwireropeto connect the load to the trolley [1]. However, without an anti-swing controller, the trolley may experience swinging due to factors such as cargo inertia, external wind, and device friction. This can greatly impact the performance of the crane, as well as pose a safety hazard. Therefore, to ensure the safe and effective operation of the crane, it is crucial to study the mechanism of crane cargo anti-swaying. This is a significant research direction in the field of crane engineering.

A robust controller can keep the system stable in the case of uncertain parameters.Additionally, it regulates the system to minimize the impact of external disturbances and parameter perturbations.

In crane operations, the load mass is not fixed and its distribution is nonuniform, resulting in a margin of error. This means that any changes in the load mass can affect the angle of the load swing. Furthermore, the operating environment of a crane is particular, and there may be some friction in the device when the lifting trolley is moving to its desired position. Therefore, it is important to design a robust controller for the bridge crane. A μ-synthesis

controller based on the DK-iterative algorithm is developed, making the lifting trolley reach the desired position within the specified time and eliminate the load swing. This method ensures that the system can resist parameter changes and external disturbances, making it robust.

2. LITERATURE REVIEW

Several domestic and international researchers conducttheoretical research on this problem, resulting in a series of significant findings. In [2], a neural network sliding mode control method based on minimal parameter learning is proposed.This method utilizes the radial basis function neural network to approximate the uncertaintymodel of the system and a good result is obtained. For the crane control system, which is characterized by nonlinearity, strong coupling, and under-actuation, Deng [3] designs a linear Active Disturbance Rejection Controller (ADRC) and compares its performance with that of the LQR control. The results show that the ADRC outperformed the LQR regarding performance indices.Guo [4] constructsan alternativefunctionbased on the expression of the energy function, the control algorithmis designed using the Lyapunov direct method. In order to reduce the complexity of the algorithm and reduce the external parameters that the algorithm relies on, a couplingcontrol signal is defined and the candidate function is reconstructed. Ultimatelythe position tracking controller and the speed trackingcontrollerare designed.In[5],Model Predictive Control (MPC) is proposed for controlling the bridge crane. This approach not only considers energy efficiency and safety but alsoconsidersstability and robustness.To minimize load swing in cranes, the authors propose a Linear Quadratic Gaussian (LQG) optimal control in [6]. The algorithm integrates the second derivative of the state variables into the LQG Common Criteria performance metrics for control and estimation, this allows for the use of additional weight to reduce the swing angle.In [7], the authors use adaptive control for a bridge crane system, employing adaptive laws to estimate unknown system parameters, friction, and load mass. These estimates are then used to calculate the control force applied to the lifting trolley.This method enables precise positioning of the trolley and eliminates the residual swing angle of the load. Liu et al. [8] propose a Non-Singular Terminal Sliding Mode Controller (NTSMC) based on neural networks for a 3D bridge crane with a double-swing structure. The controller can achieve positioning and anti-sway control of the lifting trolley by tracking a planned smooth S-shaped trajectory.

About robust control strategy, in [9], the control problems of the single-control-input and double-control-input systems for a double-pendulum structure overhead crane are investigated, and an optimal robust controller is designed using μ-synthesis. By utilizing dual control inputs, the controller can achieve positioning and pendulum angle suppression with remarkable speed. In [10], Mohammad and coworkers modeled the bridge crane as a five degree-of-freedom system. They take the equivalent mass in three different directions of the trolley, the bridge frame,and the load as uncertain parameters to design a μ-optimal robust controller. The proposed controller is applied to the original nonlinear system and simulation results demonstrate that this controller satisfies the control objectives well and has robust performance.

Some scholars propose synthesizing two intelligent control strategies to improve the crane control system's robustness. In [11], the author combines fuzzy sliding mode control with variable theory domain adaptive fuzzy control design. In [12], a researcher synthesizes fuzzy control and artificial neural network control to enhance the system's robustness and overcome the subjectivity of the selection of fuzzy rules and membership functions of a single fuzzy controller.

In this paper, a μ-synthesis robust controller is designed to address performance issues caused by an uncertain model.The load mass of the bridge crane and the friction coefficients of the steel rail are taken as the parameteruncertainties, and the uncertain model of the system is established.The appropriate performance weight and input weight functions are then designed for the closed-loop system by a concluded procedure.The relationship between the weight-function parameters and the resulting performance is analyzed.The DK-iteration algorithm is applied to solve for the μ-synthesis controller. Simulation verification is conducted to plot the response curves of the closed-loop control system and obtain analytical conclusions for the trolley position and load swing angle.To test the robustness of the system, a series of simulations is performed using different perturbation parameters. The results show that these curves are consistent with the curves of the nominal model, and meet the system's performance requirements.

3.MATERIAL AND METHODS

3.1 Bridge Crane Model

A bridge crane is primarily made up of a metal three-dimensional(3D) frame, a bridge, a lifting trolley, electrical control equipment, steel rope, and a load suspended from the trolley. The linearized model of a 3D bridge crane from [13] is quoted in equation (1).This is a simplified experimental equipment based on the actual mechanical structure of the 3D crane, as shown in Fig. 1.

Fig. 1. Experimental equipment of the 3D bridge crane

$$\begin{cases} (M_x + m)\ddot{x} + m\theta_x\ddot{l} + ml\ddot{\theta}_x = f_x - D_x\dot{x} \\ l\ddot{\theta}_x + \ddot{x} + g\theta_x = 0 \\ (M_y + m)\ddot{y} + m\theta_y\ddot{l} + ml\ddot{\theta}_y = f_y - D_y\dot{y} \\ l\ddot{\theta}_y + \ddot{y} + g\theta_y = 0 \\ m\theta_x\ddot{x} + m\theta_y\ddot{y} + m\ddot{l} - mg = f_l - D_l\dot{l} \end{cases} \quad (1)$$

The symbol denotationfor the bridge crane is presented in Table 1.

Table 1. Symbol denotation

symbol	meaning
x	Thedisplacement of the lifting trolley in the X direction
y	Thedisplacement of the lifting trolley in the Y direction
M_x	The equivalent mass of the lifting trolley in the X direction
M_y	The equivalent mass of the lifting trolley in the Y direction
l	The length of thesteel rope
m	The mass of the load
f_x	The force on the trolley along the X direction
f_y	The force on the trolley along the Y direction
f_l	The load gravity in the Z direction
D_x	The damping coefficientin the X direction
D_y	The damping coefficientin the Y direction
D_l	The damping coefficientin the Z direction
θ_y	The angle between the steel rope and the XZ plane
θ_x	The angle between the projection of the steel rope in the XZ plane and the negative direction of the Z-axis

The mass of the steel rope is negligible and the length of the steel rope is constant, represented by $\ddot{l} = \dot{l} = 0$. The linear model in the XY two-dimensional direction is obtained from equation (1) as follows:

$$\begin{cases} (M_x + m)\ddot{x} + ml\ddot{\theta}_x = f_x - D_x\dot{x} \\ l\ddot{\theta}_x + \ddot{x} + g\theta_x = 0 \\ (M_y + m)\ddot{y} + ml\ddot{\theta}_y = f_y - D_y\dot{y} \\ l\ddot{\theta}_y + \ddot{y} + g\theta_y = 0 \end{cases} \quad (2)$$

The state variablesare defined as

$$X = [x \quad \dot{x} \quad \theta_x \quad \dot{\theta}_x \quad y \quad \dot{y} \quad \theta_y \quad \dot{\theta}_y]^T \quad (3)$$

The input quantity u and output quantity Y are

$$u = \begin{bmatrix} f_x & f_y \end{bmatrix}^T, Y = [x \quad \theta_x \quad y \quad \theta_y]^T \tag{4}$$

Then its state space equation can be derived from equation (2)

$$\begin{bmatrix} X \\ Y \end{bmatrix} = \begin{bmatrix} A & B \\ C & D \end{bmatrix} \begin{bmatrix} X \\ u \end{bmatrix} + \begin{bmatrix} \Delta_A A & \Delta_B B \\ \Delta_C C & \Delta_D D \end{bmatrix} \begin{bmatrix} X \\ u \end{bmatrix} \tag{5}$$

With $\Delta_A, \Delta_B, \Delta_C, \Delta_D$ are the perturbationsfor the associated matrices.

$$A = \begin{bmatrix} 0 & 1 & 0 & 0 & 0 & 0 & 0 & 0 \\ 0 & \frac{-D_x}{M_x} & \frac{mg}{M_x} & 0 & 0 & 0 & 0 & 0 \\ 0 & 0 & 0 & 1 & 0 & 0 & 0 & 0 \\ 0 & \frac{D_x}{M_x l} & \frac{-(M_x+m)g}{M_x l} & 0 & 0 & 0 & 0 & 0 \\ 0 & 0 & 0 & 0 & 0 & 1 & 0 & 0 \\ 0 & 0 & 0 & 0 & 0 & \frac{-D_y}{M_y} & \frac{mg}{M_y} & 0 \\ 0 & 0 & 0 & 0 & 0 & 0 & 0 & 1 \\ 0 & 0 & 0 & 0 & 0 & \frac{D_y}{M_y l} & \frac{-(M_y+m)g}{M_y l} & 0 \end{bmatrix},$$

$$B = \begin{bmatrix} 0 & \frac{1}{M_x} & 0 & \frac{-1}{M_x l} & 0 & 0 & 0 & 0 \\ 0 & 0 & 0 & 0 & 0 & \frac{1}{M_y} & 0 & \frac{-1}{M_y l} \end{bmatrix}^T, \tag{6}$$

$$C = \begin{bmatrix} 1 & 0 & 0 & 0 & 0 & 0 & 0 & 0 \\ 0 & 0 & 1 & 0 & 0 & 0 & 0 & 0 \\ 0 & 0 & 0 & 0 & 1 & 0 & 0 & 0 \\ 0 & 0 & 0 & 0 & 0 & 0 & 1 & 0 \end{bmatrix}, D = 0$$

The nominal transfer function matrix P_{mds} between u and Y is

$$P_{mds}=\begin{bmatrix} P_{11} & P_{12} & 0 & 0 \\ 0 & 0 & P_{23} & P_{24} \end{bmatrix}^T=\begin{bmatrix} \frac{x(s)}{f_x(s)} & \frac{\theta_x(s)}{f_x(s)} & 0 & 0 \\ 0 & 0 & \frac{y(s)}{f_y(s)} & \frac{\theta_y(s)}{f_y(s)} \end{bmatrix}^T \tag{7}$$

3.2 Parameter uncertainty

In conjunction with the linear model described above, theload mass m, the damping coefficient D_x and D_y areconsideredto be perturbationparameters. These parameters are bounded and stochastic. The uncertain parameters can be expressed in standard form as

$$\begin{cases} m=\bar{m}(1+r_m\delta_m) \\ D_x=\bar{D}_x(1+r_{D_x}\delta_{D_x}) \\ D_y=\bar{D}_y(1+r_{D_y}\delta_{D_y}) \end{cases} \tag{8}$$

where $\bar{m}$, $\bar{D}_x$, and $\bar{D}_y$ represent the nominal value of the parameters, and r_m, r_{D_x}, and r_{D_y} represent the maximum deviation value of uncertainty. The parameters δ_m, δ_{D_x}, and δ_{D_y} represent the perturbationvalue of the parameters, with a norm less than 1. The relationship between the state space equation of the system and these parameters is denoted as

$$\begin{aligned} &A_\delta=A+\Delta_A A=A+r_i\delta_i A,\ B_\delta=B+\Delta_B B=B+r_i\delta_i B, \\ &C_\delta=C+\Delta_C C=C+r_i\delta_i C,\ D_\delta=D+\Delta_D D=D+r_i\delta_i D,\ i=m,D_x,D_y \end{aligned} \tag{9}$$

The perturbation parameters are separated to form a diagonal uncertainty matrix, designated as $\Delta_\delta=diag(\delta_m,\delta_{D_x},\delta_{D_y})$, itis subsequently feedback-connected to the nominal system P_{mds}. This is known as the upper LFT form of P_{mds} and Δ_δ, referred to as the uncertain model $P=F_u(P_{mds},\Delta_\delta)$, as shown in Fig. 2.Where Δ_δ is stable and indeterminate, but it satisfies the norm condition

$$\left\|\Delta_\delta\right\|_\infty\le 1 \tag{10}$$

$$y_\delta=\begin{bmatrix} y_m & y_{D_x} & y_{D_y} \end{bmatrix}^T,\ u_\delta=\begin{bmatrix} u_m & u_{D_x} & u_{D_y} \end{bmatrix}^T \tag{11}$$

$$u_\delta=\Delta_\delta y_\delta \tag{12}$$

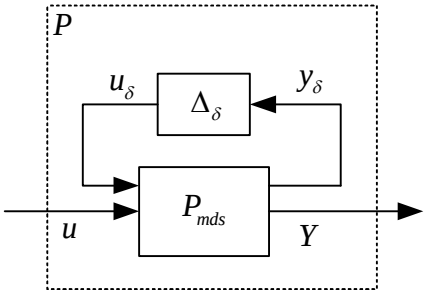

Fig.2.Upper LFT of the bridge crane system

3.3 Closed-Loop Control System of Bridge Crane

Fig. 3 illustrates the closed-loop structure of the bridge crane control system, which includes the necessary weight functions for the design. The closed-loop transfer functions both from output disturbance d to output y_d , and from reference input r to tracking error e are sensitivity functions

$$S = (I_4 + PK)^{-1} \tag{13}$$

The closed-loop transfer function from reference input r to output y_d is the complementary sensitivity function

$$T = PK(I_4 + PK)^{-1} \tag{14}$$

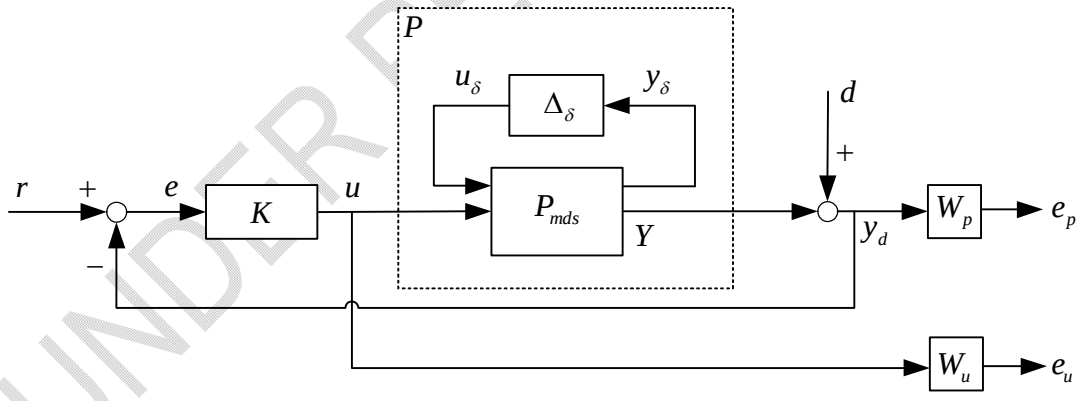

Fig. 3. Closed-loop structure of bridge crane control system

To ensure that the closed-loop system meets the required performance standards, a weight function W_p is introduced at y_d . Additionally, $1/W_P$ serves as an upper bound for the value of S [14], the performance requirement becomes

$$S(j\omega) < 1/W_p(j\omega), \forall \omega \tag{15}$$

$$W_p S < 1, \forall \omega \tag{16}$$

$$\left\| W_p S \right\|_\infty < 1 \tag{17}$$

In order to limit the model input values f_x and f_y, which is equivalent to constrain $u = KS(r-d)$, an input weight function W_u is introduced. The upper bound of the amplitude of KS is set to $1/W_u$. The robust performance of the closed-loop system can be clearlydescribed as the peak value of the closed-loop transfer function being less than 1 for the uncertain model P in all frequency ranges with the following constraint

$$\left\| \begin{matrix} W_p S(P) \\ W_u KS(P) \end{matrix} \right\|_\infty < 1 \tag{18}$$

3.4 Selection of the Weight Function

The weight functions W_p and W_u are used to indicate the relative impact of performance and input requirements in different frequency ranges. The typical weight function W_p is expressed in [14] and [15].

$$W_P(s) = \frac{s/M + \omega_B^*}{s + \omega_B^* A} \tag{19}$$

Parameters A, M and ω_B^* are related tosteadystate tracking error, maximum peak magnitude and time response speed.To improve the tracking accuracy of each controlled output, the sensitivity function should be as small as possible, so the weight function should contain an integral term. For this control object, the steadystate trackingerror is not required to be 0, so setting the weight function can generate a limited gain in the low-frequency band. By adjusting W_p, it has been found that limited attenuation in the high-frequency band is beneficial in reducing the maximum peak amplitude.In the low-frequency band, the amplitude of $1/W_P(j\omega)$ is equal to A, while in the high-frequency band, it is equal to $M \geq 1$. If A increased, the steadystate tracking error of the output response curve will also increase. If M increased, the maximum peak of the response curve will also increase. At frequency ω_B^*, the asymptote crosses 1, which is approximately the required bandwidth and is related to the time response speed. Increasing ω_B^* will result in a faster response speed for the trolley displacement and load swing angle.

At the high-frequency band, the input weight function hasa small gain to reduce the controller's gain and avoid input saturation.For precise control in the low-frequency band, W_u is best used in the following form

$$W_u(s) = \frac{s}{s + w_1} \tag{20}$$

where w_1 is approximately equal to the closed-loop bandwidth.The smaller the w_1, the smaller the input force, and the large oscillation of the load swing angle.If w_1 is too large, the nominal performance will be affected.The robustness performance cannot meet the requirements if w_1 is too small.

The performance requirements for the designed system include a maximum overshoot of 10% displacement, a stabilization time of 5 seconds or less, a maximum tracking error of 5%, and a maximum input force of 20N.Thevalues are taken through repeated debugging as follows

$$W_p = \mathrm{diag}\left\{\frac{s/2.5+0.55}{s+0.0055}, \frac{s/1.1111+0.2163}{s+0.8652}, \frac{s/2.5+0.64}{s+0.0122}, \frac{s/1.1111+0.2163}{s+0.8652}\right\} \quad (21)$$

$$W_u = \mathrm{diag}\left\{\frac{s}{s+1000}, \frac{s}{s+1000}\right\} \quad (22)$$

If any parameter of the model changes, or the maximum deviation value of uncertainties in (8) changes, the appropriate weight functions need to be re-selected.

Remark: It can be seen from (2) that there is a linear relationship between the load swing angle and the trolley acceleration, which cannot be ignored when W_P is valued. Using the above-summarized relationships and laws, the weight functions W_{P1} and W_{P3} of P_{11} and P_{23} (the transfer functions of the trolley displacement and input force in the X and Y directions)in(7) are taken.

$$W_p = diag\{W_{P1}, W_{P2}, W_{P3}, W_{P4}\} = diag\left\{\frac{s/1.8+0.6}{s+0.0054}, 1, \frac{s/0.7+0.64}{s+0.0122}, 1\right\} \quad (23)$$

The minimum μupper bound of the closed-loop system is 1.13, which does not meet the robust performance of the(27), and the nominal performances exceed the required value. Further, the weight functions W_{P2} and W_{P4} about P_{12} and P_{24} are set. Finally,the (21) is selected using the above debugging rules. w_1 is greater than 195 in W_u, the minimum μ upper bound of the closed-loop system will be less than 1, which satisfies robust performance ofthe (27).

3.5 Linear Fractional Transformation and System Performance Description

The system structure is transformed to analyze the robust stability and robust performance of the MIMO system under multiple disturbances. The controller K is extracted from the given system structure in Fig. 4 to obtain the generalized object G. The block diagram for the synthesized controller is shown in Fig. 4.

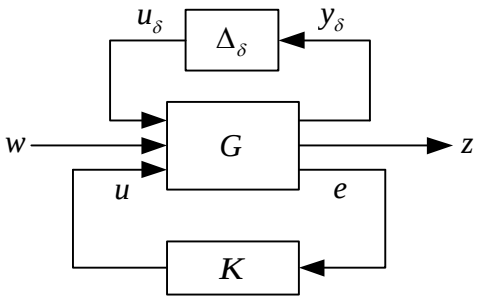

Fig. 4.Block diagram for the synthesized controller

with

$$r = \begin{bmatrix} r_x & r_{\theta_x} & r_y & r_{\theta_y} \end{bmatrix}^T, d = \begin{bmatrix} d_x & d_{g_x} & d_y & d_{\theta_y} \end{bmatrix}^T,$$

$$e = r - y_d = r - Y - d = \begin{bmatrix} e_1 & e_2 & e_3 & e_4 \end{bmatrix}^T, e_p = \begin{bmatrix} e_x & e_{\theta_x} & e_y & e_{\theta_y} \end{bmatrix}^T,$$

$$e_u = \begin{bmatrix} e_{f_x} \\ e_{f_y} \end{bmatrix}, w = \begin{bmatrix} r \\ d \end{bmatrix}, z = \begin{bmatrix} e_p \\ e_u \end{bmatrix}, G = \begin{bmatrix} G_{11} & G_{12} \\ G_{21} & G_{22} \end{bmatrix}.$$

Fig. 5 illustrates the structure of $N\Delta_\delta$ for robustness analysis, with the nominal system N being the lower LFTof G and K.

$$N = F_l(G,K) \triangleq G_{11} + G_{12}K(I - G_{22}K)^{-1}G_{21} = \begin{bmatrix} N_{11} & N_{12} \\ N_{21} & N_{22} \end{bmatrix} \tag{24}$$

The structure of $M\Delta_\delta$, shown in Fig. 6, is used for robust stability analysis, $M = N_{11}$. It represents the transfer function from u_δ to y_δ.The uncertain closed-loop transfer function from w to z can be represented by the upper LFT of N and Δ_δ.

$$F = F_u(N,\Delta_\delta) \triangleq N_{22} + N_{21}\Delta_\delta(I - N_{11}\Delta_\delta)^{-1}N_{12} \tag{25}$$

To analyze robust performance using structural singular values μ, a virtual uncertainty sub-block Δ_p must be introduced in the uncertainty block. This sub-block is afull complex perturbation matrix and represents the H_∞ performance specification. The uncertainty structure becomes H_∞

$$\Delta = \begin{bmatrix} \Delta_\delta & 0 \\ 0 & \Delta_p \end{bmatrix} \tag{26}$$

The robust performance requirements for all allowable perturbations are defined as $\|F\|_\infty \le 1$ in (25).The nominal stability (NS), nominal performance (NP), robust stability (RS), and robust performance (RP) are obtained as

$$\begin{aligned}
&\text{NS} \Leftrightarrow N \text{ is internally stable}, \\
&\text{NP} \Leftrightarrow \bar{\sigma}(N_{22}) = \mu_{\Delta_P} < 1, \ \forall \omega, \text{ and NS}, \\
&\text{RS} \Leftrightarrow \mu_{\Delta_\delta}(N_{11}) < 1, \ \forall \omega, \text{ and NS}, \\
&\text{RP} \Leftrightarrow \mu_{\Delta}(N) < 1, \ \ \forall \omega, \text{ and NS}.
\end{aligned} \tag{27}$$

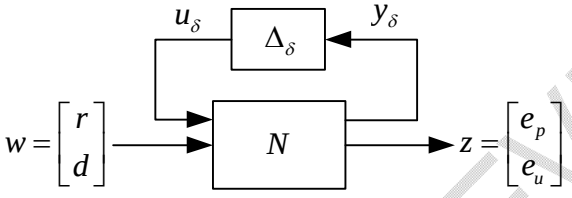

Fig. 5. $N\Delta_\delta$ **-Structure Block Diagram**

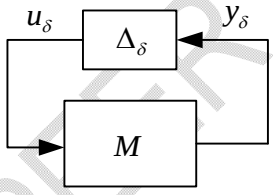

Fig. 6. $M\Delta_\delta$ **-Structure Block Diagram**

3.6 μ-Synthesis and DK-iteration

The definition of structured singular value is provided in [16]. For a given controller, μ is used to analyze RP effectively.μ-synthesis problem refers to finding the controller that minimizes the μ. According to the structure shown in Fig. 6, the appropriate controller is found by minimizing H_∞ norm from w to z , i.e., $\|F\|_\infty$ in (25), which is usually solved by the DK-iteration[16].

The upper bound $\mu(N) \le \min \bar{\sigma}(DND^{-1})$ on the structured singular value is solved using the DK-iteration method, which minimizes $\left\|DN(K)D^{-1}\right\|_\infty < 1$ by alternately changing K and D , where $D(s)$ is the scale transformation matrix, as follows:

i) Kstep: $D(s)$ remain unchanged, the controller K is obtained by solving $\min_K \left\|DN(K)D^{-1}\right\|_\infty$.

ii) D step: Find $D(j\omega)$ such that $\bar{\sigma}(DND^{-1}(j\omega))$ is minimized at each frequency when N is unaltered.

iii) Fit the amplitude of each element in $D(j\omega)$ so that $D(s)$ is a stable minimum phase transfer function and return to the K step. Next, iterate alternately until $\left\|DN(K)D^{-1}\right\|_{\infty}<1$ or H_{∞} norm is no longer decreasing.

The generalized control object is obtained using the *connect* command for the controlled object $P(s)$ and all the weight functions. Then, the *musyn* function in the MATLAB robust control toolbox is utilized to solve the controller.

4.RESULTS AND DISCUSSION

The experimentalbridge crane trajectory tracking control issimulated with the following parameters: $M_y=16\mathrm{Kg}$, $M_x=6\mathrm{Kg}$, $l=1\mathrm{m}$, $g=9.8\mathrm{m/s}^2$, $\bar{m}=2\mathrm{Kg}$, $\bar{D}_x\approx 20\mathrm{Kg/s}$, $\bar{D}_y\approx 20\mathrm{Kg/s}$, $r_m=0.3$, $r_{D_x}=r_{D_y}=0.2$ .After five iterations,the closed-loop maximum structured singular value of 0.904 is obtained for the μ-synthesis controller K . This indicates that the closed-loop system can tolerate a maximum uncertainty error of 1/0.904 times the specified uncertainty. The controller can achieve RPof theclosed-loop system in all parameter uncertainty ranges. The maximum singular value curves of the closed-loop system under nominal condition and the worst peak gain case are shown in Fig. 7.

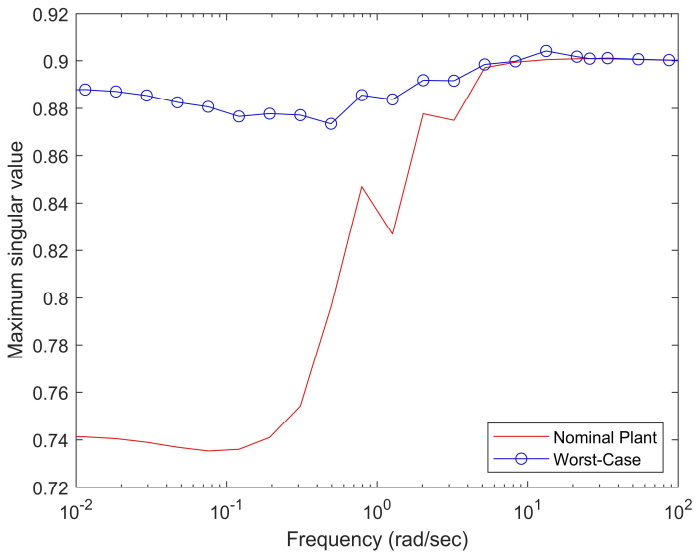

Fig.7.Maximum singular value

Through the simulation experiment, the displacement curveof the lifting trolley and the swing angle amplitude curve of the load are obtainedin the X and Y directions, and compared with the LQR controller.

The inputtracking responsecurvesof the uncertain system at the designated position $x=1\mathrm{m}$ and $y=1\mathrm{m}$ of the trolley,and the desired swing angles $\theta_x=0°$ and $\theta_y=0°$ of the load are shown in Fig. 8. Thetracking curves in the X direction are illustrated in Fig. 8(a),and the

trolley displacement with the μ-synthesis controller arrives at the specified position in 3.3s, with the maximal swing angle within 6°, and converges to about 0° in 3s.The trolley displacement with the LQR controller is tracked more slowly, reaching about 1m in 8s, but the amplitude of the pendulum angle of the load varies little, and the maximal pendulum angle is only 2.93°, which also converges to the designated pendulum angle in 3s.

Fig. 8(b) shows the tracking curves in the Y direction.The trolley displacement under the μ-synthesis control reaches the appointed value in 2.7s, and the pendulum angle converges to about 0° in 3s. In comparison, the displacement under the LQR control reaches the designated value in 8s, and the pendulum angle reaches the assigned value in 2.7s. In contrast, the response speed of the μ-synthesis control is faster.The lifting trolley can get the specified position accurately, and the swing angle of the loadfluctuates a lot, but it is within the safety allowable range, significantly improving the tracking performance compared with that of the LQR controller.

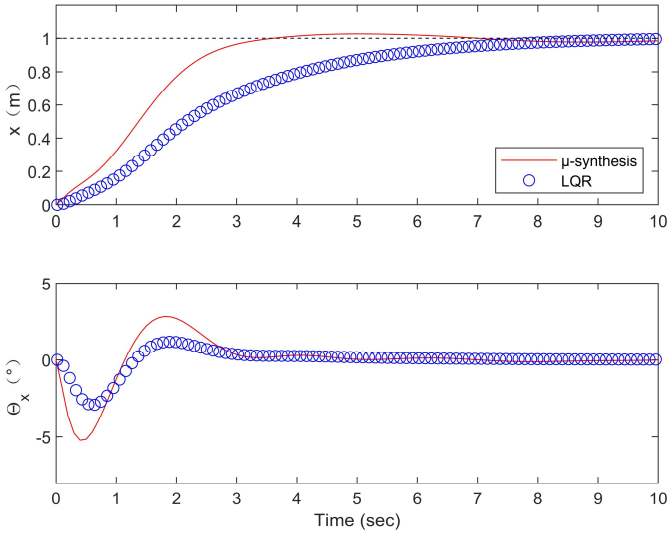

Fig.8a.Tracking performance in the X direction

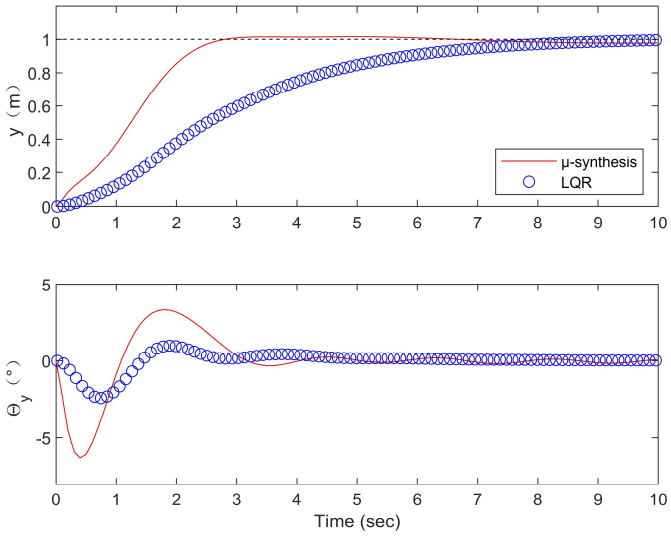

Fig.8b.Tracking performance in the Y direction

The variation of the input-force when using the μ-synthesis control is shown in Fig.9.The maximum input driving force of the lifting trolleyin the X direction is 11.8N, the common input-force of both the bridge and the trolleyin the Y direction is 17.59N, the amplitude of which is within the permissible input-force requirement. The above results show that the tracking performance of the bridge crane using μ-synthesis controller is better.

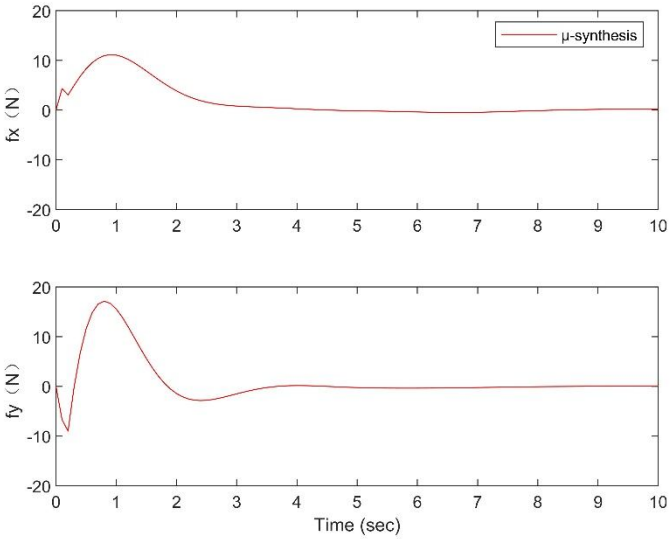

Fig.9. Input-forces during reference input tracking

Fig.10shows the simulation curves of the closed-loop system for output disturbance rejection. Considering the frictionforce of the device and wind force, the displacement of the trolley may deviate from the expected position, and the load will also be disturbed to produce

the swing angle. Therefore, 0.1rad disturbance input is set for θ_x and θ_y, and the displacement disturbance inputof 0.2 m is set for x and y. Corresponding to the closed-loop structure of Fig. 4, set

$$d = \begin{bmatrix} d_x & d_{\vartheta_x} & d_y & d_{\theta_y} \end{bmatrix}^T = \begin{bmatrix} 0.2 & 0.1 & 0.2 & 0.1 \end{bmatrix}^T .$$

As can be seen from Fig. 10a and Fig. 10b, in the presence of output disturbance, regardless of the X, and Y direction, the curve of trolley displacement and the swing-angle curve of the load converge to 0 in about 3s by using μ-synthesis controller, and the effect of eliminating the swing is better. Inthe LQR control process, trolley displacement and swing angle changes are pronounced. Eliminating the pendulum can be realized in the time required, but the pendulum angle is large, beyond the safety requirement. The results demonstrate that μ-synthesis controller exhibits superior disturbance rejection performance.

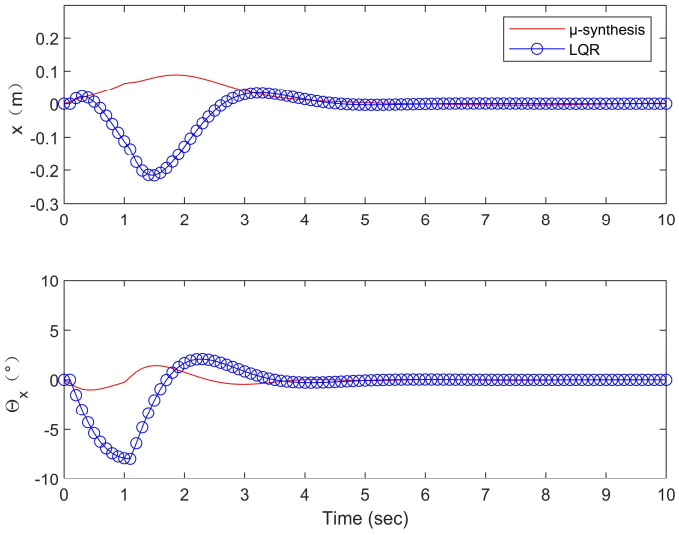

Fig.10a. Disturbance rejectionin the X direction

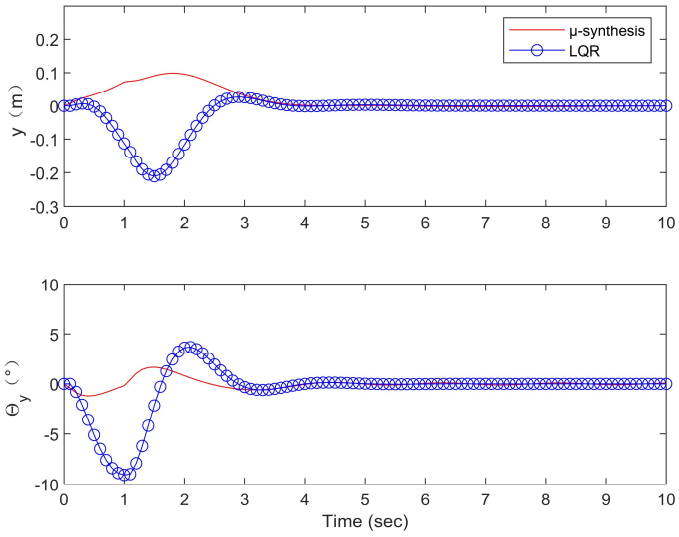

Fig.10b. Disturbance rejectionin the Y direction

Fig. 11 shows the input-force variation of the trolley when the μ-synthesis controller realizes the disturbance rejection. In the event of output disturbance, the maximum value of the trolley input-force is between ±5N, and only lesser force is needed to maintain the stability of the load swing angle.

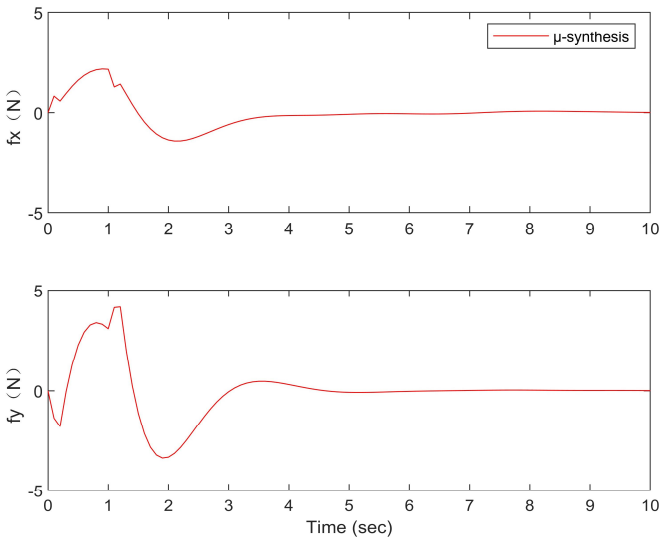

Fig.11. Input-forces during disturbance rejection

The robust performance of the closed-loop control system is verified in the time domain. To demonstrate the response performance of the μ-synthesis controller to the change of system parameters, the uncertainty parameter valuesare adjusted within the range of deviation values in (8).The load mass m isadopted with an accuracy of 0.2kg, and the damping

coefficients D_x and D_y areboth given with an accuracy of 1. The tracking curves of different parameter perturbationsare obtained, as shown in Fig. 12, and the disturbance rejection curves of parameter perturbations are shown in Fig. 13.

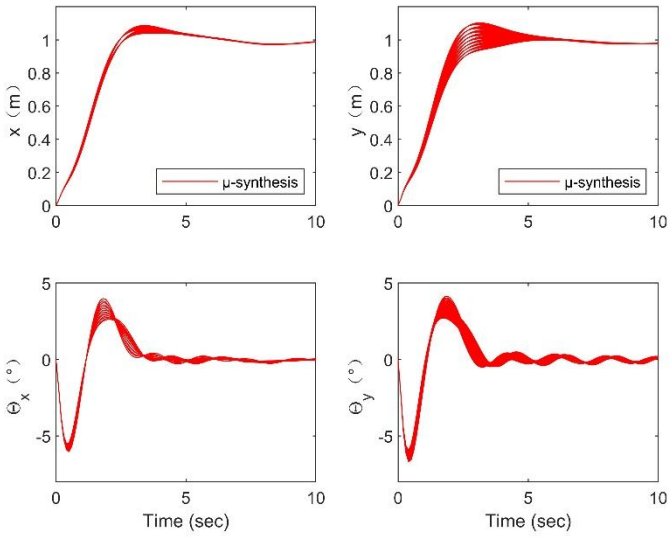

Fig.12. Tracking performancefrom perturbationparameters

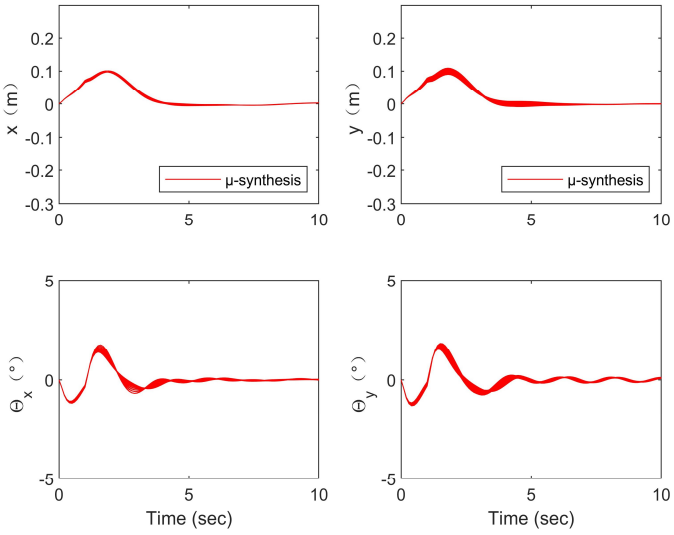

Fig.13.Disturbance rejectionfrom perturbation parameters

Compared to the control results under the nominal model simulated above, the curves after changing the parameters are similar to it, hencethe better robustness of the designed μ-synthesis controller is verified.

5. CONCLUSION

Based on the robust control theory, a μ-synthesis robust controller is designed for the control problem of a bridge crane system containing uncertaintiesincluding the model parameter perturbations, output disturbances, and input limit in amplitude. Considering the variation of load mass and the fluctuation of the damping coefficient of the lifting trolley during the moving process, the uncertainty bounds are given, and a reasonable closed-loop control structure of the bridge crane is composed. The relationship between the parameters of the weight function and the steady state error, response speed, and maximum peak value of the system is given, and the appropriate performance weight function and input weight function are selected. The simulation results show that the controller can realize the positioning control and rapid swing elimination of the bridge crane system with fixed rope length and two degrees-of-freedom. The three perturbation parameters take different values respectively, the closed-loop system is verified to be RS within the parameter perturbation range, and it has a better RP to the output disturbance.

Disclaimer (Artificial intelligence)

Authors hereby declare that NO generative AI technologies such as Large Language Models (ChatGPT, COPILOT, etc) and text-to-image generators have been used during writing or editing of manuscripts.

REFERENCES

1. HUANG Dawei, LI Feng, MAO Wenjie. Modern lifting and transportation machinery [M]. Beijing: Chemical Industry Press; 2006.
2. SUN Jiajun, CAI Lin, GUO Qihang, LIU Huikang. Neural network sliding mode control of bridge crane in 3D motion mode[J/OL].Control Theory and Applications. 2023;1-9. Accessed10 July 2024.
Available:http://kns.cnki.net/kcms/detail/44.1240.TP.20231114.1414.054.html.
3. DENG Wei. Three-dimensional crane control based on linear active disturbance rejection theory[J]. Digital Technology and Application. 2020;38(06):161-162.
4. GUO Xiang. Design of power assist crane system and anti-swing control[D]. Yanshan University;2021.
5. Wu Zhou, Xia Xiaohua, Zhu Bing. Model predictive control for improving operational efficiency of overhead cranes[J]. Nonlinear Dynamics. 2015;79(4): 2639-2657.
6. PittayaPannil, Krit Smerpitak, Visitsak La orlao, ThanitTrisuwannawat. Load swing control of an overhead crane[C]. International Conference on Control, Automation and Systems. 2010;1926-1929.
7. Quoc Chi Nguyen, Ha-Quang-Thinh Ngo, Won-Ho Kim. Nonlinear adaptive control of a 3D overhead crane[C]. IEICE Transactionson Communications. 2015;41-47.
8. LIU Jiahui, CHENG Wenming, CHEN Qingrong, DU Run. Neural network sliding mode control for double-pendulum bridge crane with input saturation[J]. Control Engineering of China. 2024;31(4):687-694.
9. Hamed Moradi, Gholamreza Vossoughi. State estimation, positioning and anti-swing robust control of traveling crane-lifter system[J]. Applied Mathematical Modelling. 2015;39(22):6990-7007.
10.Khoshnazar, M., Barjini, A.H. & Moradi, H. Using a robust mu-synthesis based controller to eliminate the adverse effects of uncertainties and external disturbances in nonlinear 3D overhead cranes with hoisting mechanism. Meccanica (2024). https://doi.org/10.1007/s11012-024-01846-7

11. JIAO Chenhui. The 3D crane system based on fuzzy sliding mode control[D]. Dalian University of Technology;2010.
12. WANG Junfeng. Research on anti-swing control system strategy and device of garbage grab crane[D]. South China University of Technology;2018.
13. SHI Lanting. Research on control method of bridge crane system[D]. Tianjin University of Technology and Education;2023.
14. Sigurd Skogestad, Ian Postlethwaite. Multivariable Feedback Control: Analysis and Design[M].5th ed.New York: John Wiley and Sons; 2005.
15. LIU Kangzhi, YAO Yu. Linear robust control[M]. Beijing: Science Press; 2013.
16. ZHOUKemin, Doyle John C. Essentials of Robust Control[M]. New Jersey: PrenticeHall;1998.